

Simplified Model Researches for Understanding the Complex Shock Interactions in Hypersonic Inlet Flow

Jiming Yang

Department of Modern Mechanics, University of Science and Technology of China,
Hefei, Anhui, 230026, China

Jiming Yang: jmyang@ustc.edu.cn

Abstract The paper presents some progresses of the shock wave interaction studies in author's group, with the application background of complex hypersonic inlet flow, particularly with a focus on the characterization of an inward-turning inlet flow. We start with a report of several experimental efforts, which attempted to visualize the flow features hidden in an inlet. Then the major topic is concentrated on the cowl lip, namely a simplified “V” shaped blunt leading edge, about which a severe shock interaction is discussed that is comparable to the well-known type IV interaction in the sense of peak pressure and heat flux. Another discussion is about the behaviors of a near-axisymmetric converging shock wave, which is picked up as a candidate to exhibit some typical characteristics in an inward-turning inlet that differ remarkably from the case of a 2D inlet.

1 Introduction

Shock wave interaction problem is a well-known subject for both fundamental research and development of hypersonic flight, in which a typical example might be the intake of an air-breathing hypersonic vehicle, who swallows not only the incoming flow for the propulsion, but also the nets of waves generated from the edges and/or non-uniform boundary conditions along the air passage. As the major concern of the present paper, the shock interaction problems in an inward-turning inlet are considered and discussed. Hypersonic inward-turning inlets have received considerable attention because of their advantages of high compression ratio, high mass capture rate, and small wetted area, etc.[1-3] However, due to its special structure and complicated three-dimensional inner flow, a clear characterization seems to be very challenging. Numerical simulations have showed the occurrence of strong shearing actions and shock interactions in the inward-turning inlet flow [4], although it is much more difficult to obtain a detailed insight flow structures experimentally [4,5] as compared to the conventional studies such as 2D inlet visualization.

This paper presents the progress so far in the author's group, with the efforts of using “simple” ways to clarify some important characteristics, particularly shock wave interaction behaviors that an inward-turning inlet may have out of other types of inlet. The

works are separated into three parts for easy discussion: The first part is about the experimental works, in which some attempts are put into practice to visualize as much as possible the flow features hidden in an inlet. Whereas the following two stories are focused onto two simplified models that may exhibit the unique characteristics of an inward-turning inlet flow. One is a key part of the inlet, namely the cowl lip with “V” shaped blunt leading edge, which is related to the severe shock interaction comparable to the well-known type IV shock interaction in the sense of peak pressure and heat flux. The other one is about the behaviors of a convergent shock wave, which appears typically in an inward-turning inlet and differs remarkably from that of 2D inlet.

2 Visualizing the flow hidden in an inlet

As shown Schematically in Fig.1, it is not so easy to “look” into or through the inner part of an inward-turning inlet. To extend the visual field further, quite a few efforts were tested in the author’s group. Here we introduce some of our attempts and pick up a few results which are not very disappointed.

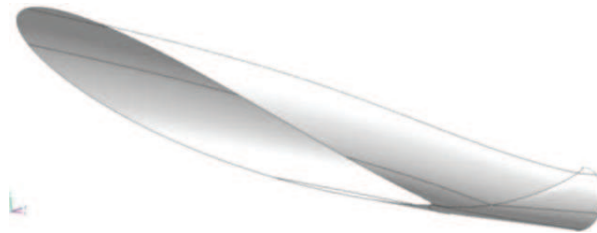


Fig. 1 Schematic configuration of a typical inward-turning inlet[4]

The first attempt was to visualize the flow with planar laser scattering method in a shock tunnel, and condensed H₂O particles were used as tracers at proper conditions. An example of visualizing the curved shock generated by the forebody compression surface is shown in Fig. 2 [6], in which a truncated inlet model produced by a 3D printer, was used for a back-view photography. As can be recognized from the photo that the brighter area illuminated by the laser sheet is the compressed flow behind the shock wave. Therefore, the curved shock front can be readily obtained through searching the edge between the bright and dark areas.

In Fig. 3, a “cut-through” view of the isolator is shown, together with a CFD result of Mach number distribution. The bright part in the photo represents high speed core flow, and the surrounding dark part is the low speed flow with relatively high temperature where the H₂O particles are evaporated and result in less illumination. A combined analysis of the experimental and numerical information infers that, the eddy-like flow at the top of the cross section is a result of the severe interaction from the cowl lip, a key part of the inlet, which will be further discussed in part 3.

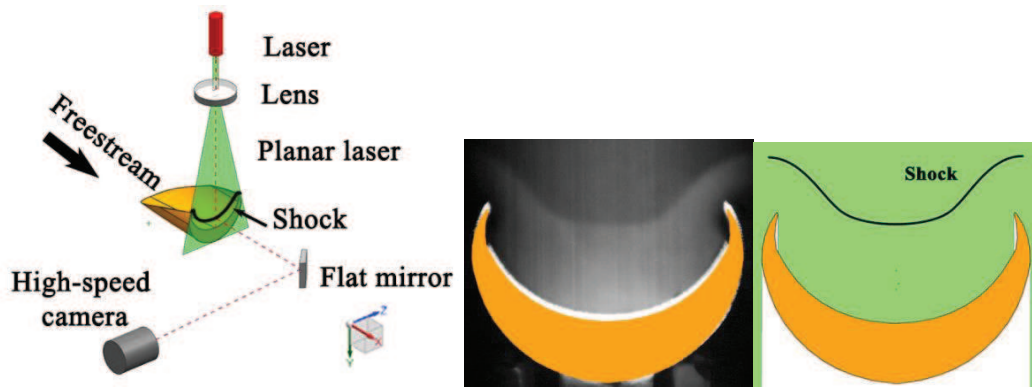


Fig. 2 Schematic truncated forebody model and scattering image of the forebody shock.

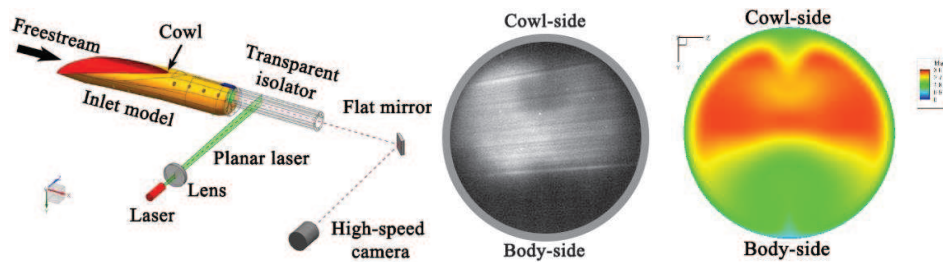
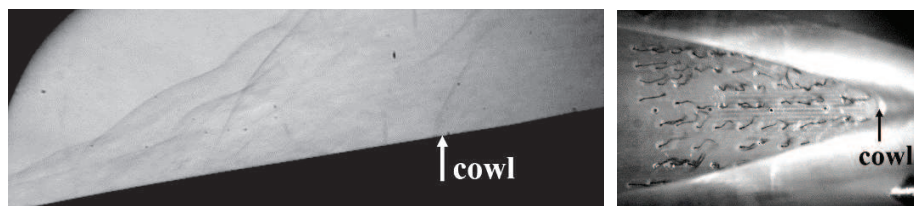


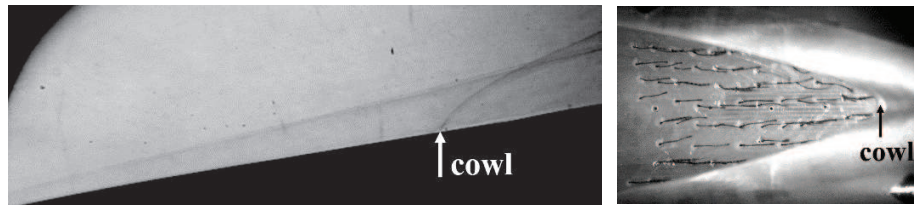
Fig. 3 Schematic “cut-through” view of isolator supplemented with numerical Mach number distribution (right) [6].

One more try need to be mentioned is a combination of high speed photography of surface tuft motion with Schlieren technique, in which two high speed cameras were used to record the motions of the surface tuft and Schlieren images, respectively, with the same synchronized time steps. So that the motion of shock wave structure can be analyzed together with the coupled motion of surface tuft.

It is shown that during an un-starting process, the tufts suddenly swing upstream while the shock waves above the cowl are spilled out towards the upstream (see the upper pair of photos in Fig. 4). On the other hand, after the inlet is re-started and the shock waves are settled down sitting stably around the inlet, the tufts also turn to direct downstream regularly (see the bottom pair of photos). Such a dynamic process is more recognizable with the help of movie animation, which is going to be presented onsite during the conference.



(a) Un-starting stage.



(b) Re-starting stage

Fig. 4 Typical images of Schlieren (side-view, left) and surface tuft (top-view, right) at un-starting and re-starting stages [7]

3 Simplified model of cow lip -- "V" shaped blunt leading edge

As an important part of inward-turning inlet, the cowl with V-shaped configuration, as can be recognized from Fig. 1 and Fig. 4, is commonly designed to allow for flow spillage during various flight conditions. In addition, blunting the leading edge is another basic demand for the reduction of peak heating to an acceptable level. However, these two requirements bring serious interaction problems to the conjunction part of the cowl, which attract our attention sufficiently. To get rid of the complexities of inner/outer coupling problems, we proposed a simplified model called "V-shaped blunt leading edge (VsBLE)" for the purpose of picking up the crucial mechanism of the interaction.

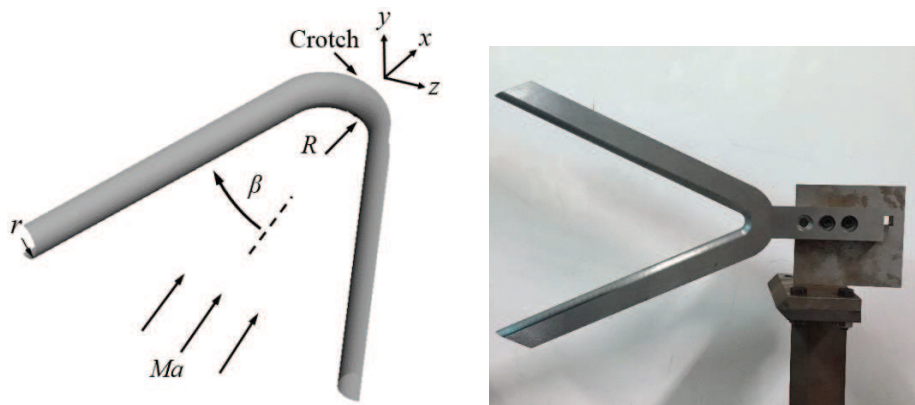


Fig. 5 Simplified model of V-shaped blunt leading edge

As shown in Fig. 5, the simplified model is characterized by a span angle β , a leading-edge bluntness r , and a radius of curvature of the crotch R . Therefore the variables β , r , and R are supposed to be the key factors which dominate the shock interaction under a certain flow condition.

Typical experimental results are collected in Fig. 6. As a summary, a series of complicated wave configurations are observed at the crotch and categorized as regular reflection (type A), Mach reflection (type B), and regular reflection from the same family (type C), according to the primary shock interaction layouts [8]. For types B and C, shear layers bounded jets are formed and spontaneously converges inward by the contraction of

the crotch, followed by the collision of the jets near the stagnation point that results in a reverse flow. Severe oscillations of the primary shocks are exhibited (particularly type B) since the downstream reverse flow can impact on the primary Mach stem ahead of the stagnation point.

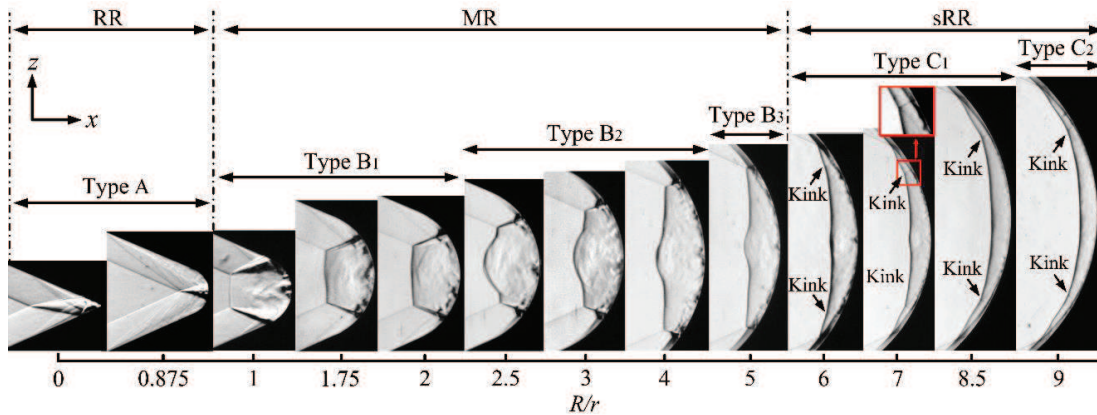


Fig. 6 Schlieren images of various interaction types [8]

One serious concern is the peak heating suffered from the shock interaction. Figure 7 shows how the surface heat flux is affected by the leading-edge bluntness r , in which the symbols denote the numerical results of the stagnation-point heat flux (red dots) and the peak values in the surface heat flux q_{max} (blue triangles) of the leading edge, and the curve represents the classical prediction based on the Fay and Riddell's theory. It is well known from Fay and Riddell's theory that the stagnation heat flux scales inversely with the square root of the leading-edge bluntness r . The present results agrees fairly well if the bluntness r is small enough (region A), under a given radius of the crotch R . However, if r is increased beyond a certain level, the peak heat flux starts to climb up again remarkably, which is comparable to that of the well-known type IV shock interactions [9]. This finding needs to be emphasized since it is opposite to our conventional concept of heat protection.

The aforementioned shock interaction causes not only the severe peak heating at the crotch, but also strong interference to the flow field, which remains effective far downstream. With the help of high resolution numerical simulation, it was found that shear layers bounded supersonic jets are formed near the wall. These supersonic jets are forced inward by the contraction of the crotch, and finally collide near the stagnation point. The combined streams are diverted forward, and a reverse flow is therefore formed, which rolls flow into a counter-rotating vortex pair [10] (as shown in Fig. 8). This finding may offer a reasonable explanation for the eddy-like flow shown in Fig. 3.

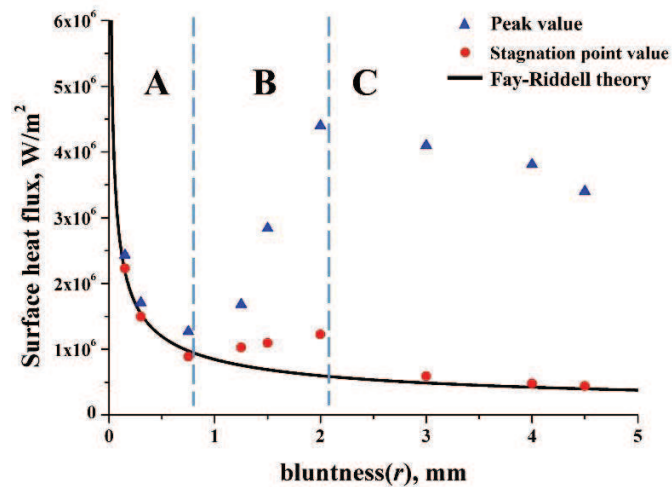


Fig. 7 Surface heat flux at different leading edge bluntness conditions[9]

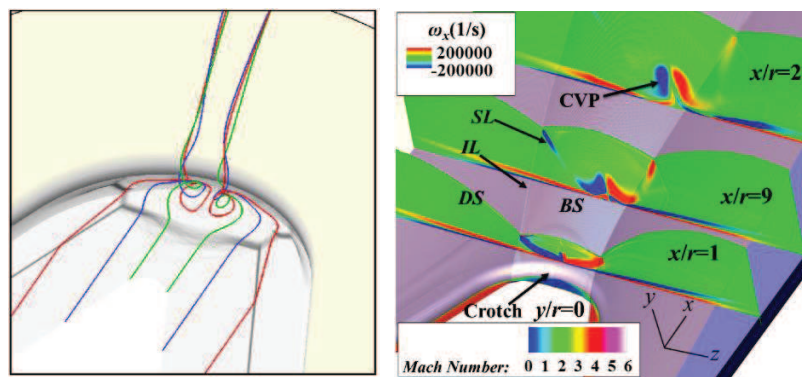


Fig. 8 Three-dimensional interference around VsBLE [10]

Therefore, it should be pointed out that the variables β , r , and R , etc., could be well arranged or optimized so that not only the peak heat flux can be reduced remarkably, but also the flow field can be much more regularly organized at the same time.

4 Behaviors of near-axisymmetric converging shock waves

In this part, we attempt to choose a couple of simplified models which may characterize the major behaviors of a curved, convergent shock wave, so that some fundamental concepts might be formed for an inward turning inlet other than that of a 2D inlet. Since studies for the case of axisymmetric shock wave are sufficient and non-axisymmetric cases are much more practical, our interest is therefore concentrated to the subject of "near-axisymmetric converging shock waves".

For the time being, two models were chosen and perform both numerically and experimentally. One is elliptical wedge with small ellipticity and the other is circular wedge facing a small angle of attack. Therefore, the former is a deviation of geometrical condition

and the latter is a mismatch of the axis with the direction of the incoming flow (as shown in Fig. 9).

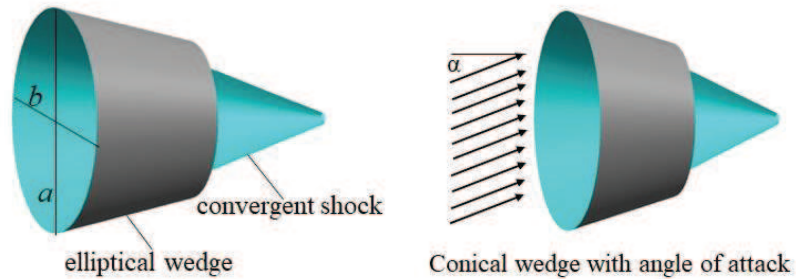
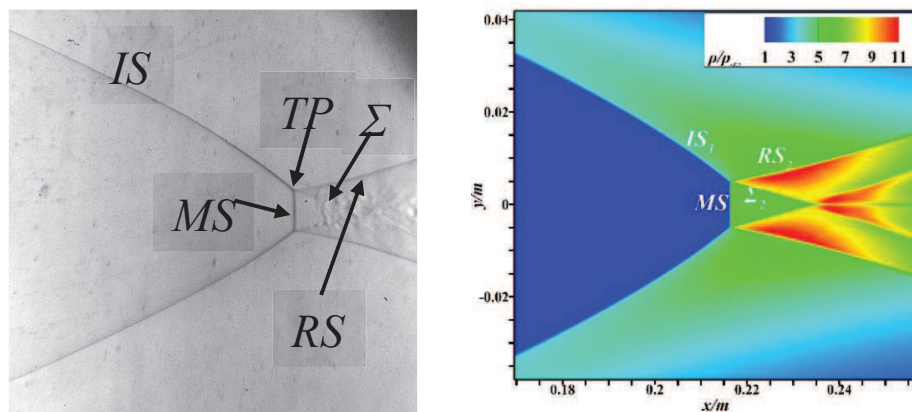
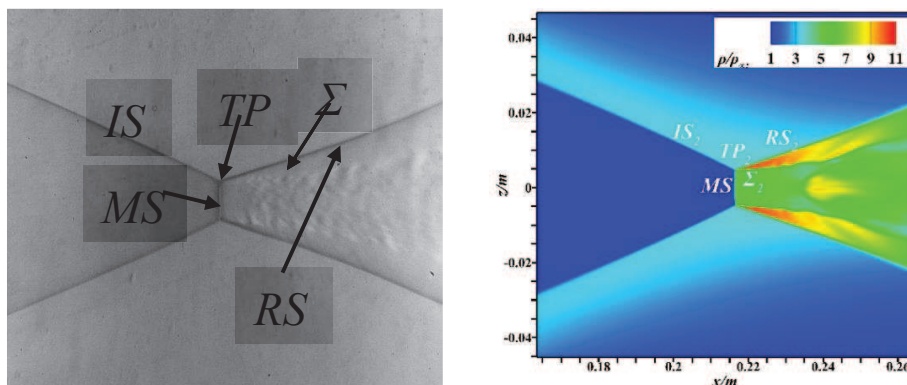


Fig. 9 Two simplified models generating near-axisymmetric converging shock wave

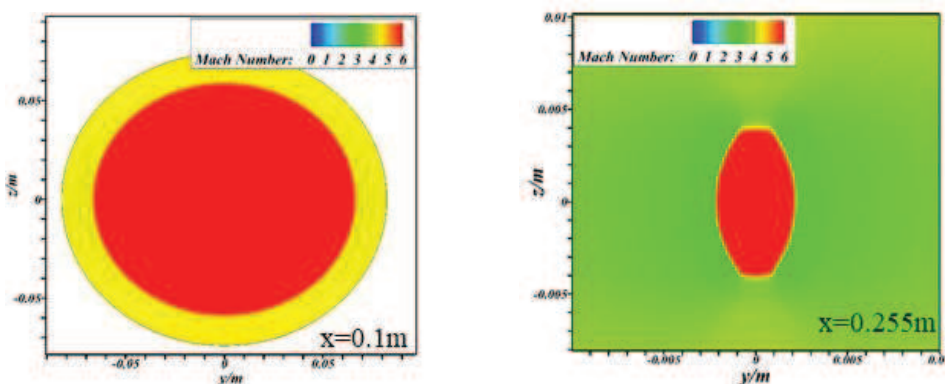
Fig. 10 shows an example of convergent shock generated with an elliptical wedge, of which the ellipticity of $b/a=0.9$. Similar to the case of axisymmetric conical shock convergence, a Mach reflection is exhibited at the center part as a termination of converging strength enhancement, although the non-axisymmetric effects are also obvious. An interesting point deserve to be mentioned is that the shear layer behind the triple point tends to be convergent on the major plane but divergent on the minor plane, which means that the reflection type of the former is direct Mach reflection and the latter is an inverse Mach reflection [11]. The non-uniform shock enhancement around the circumferential direction is also striking. The fastest strength enhancement is located at the end of the major axis, where the curvature is the highest, which can be verified through a measure that it approaches the center earlier than other part regardless of its longest distance (see the bottom of Fig. 10).



(a) Experimental Schlieren (left) and numerical density distribution (right) on the major plane



(b) Experimental Schlieren (L) and numerical density distribution (R) on the minor plane



(c) Mach number distribution on Y-Z planes at entrance (L) and near focus (R).

Fig. 10 Convergent shock generated by an elliptical wedge. $b/a=0.9$, $Ma=6$, $\delta=12^\circ$

Figure 11 shows examples of non-axisymmetric flow arising from angles of attack [12], with incoming flow $M=6.0$. At small angle of attack, although the flow features are generally similar to the case of axisymmetric one typically with Mach disk at the convergent center, different behaviors are also remarkable. It can be seen from the figure (upper) that the incident shock on the windward side passes the axis before the occurrence of the Mach reflection, which is opposite to 2D case owing to a faster shock strength enhancement on the windward. Furthermore, as a result of the flow inclination, there is not only a shrinkage in size of the Mach disk, but also a leaning forward in direction, in which the reflection type on the windward is direct Mach reflection, and that on the leeward is inverse Mach reflection [12].

When the angle of attack is increased to a certain level, it is noted that the Mach disk disappears as the non-axisymmetrical effect is strong enough, and the shock structure becomes very similar to a regular reflection, as shown in Fig. 11 (bottom). However, the area near the convergent center is far from a simple intersection of the incident shock followed by a reflected shock, and more discussions are presented in [12].

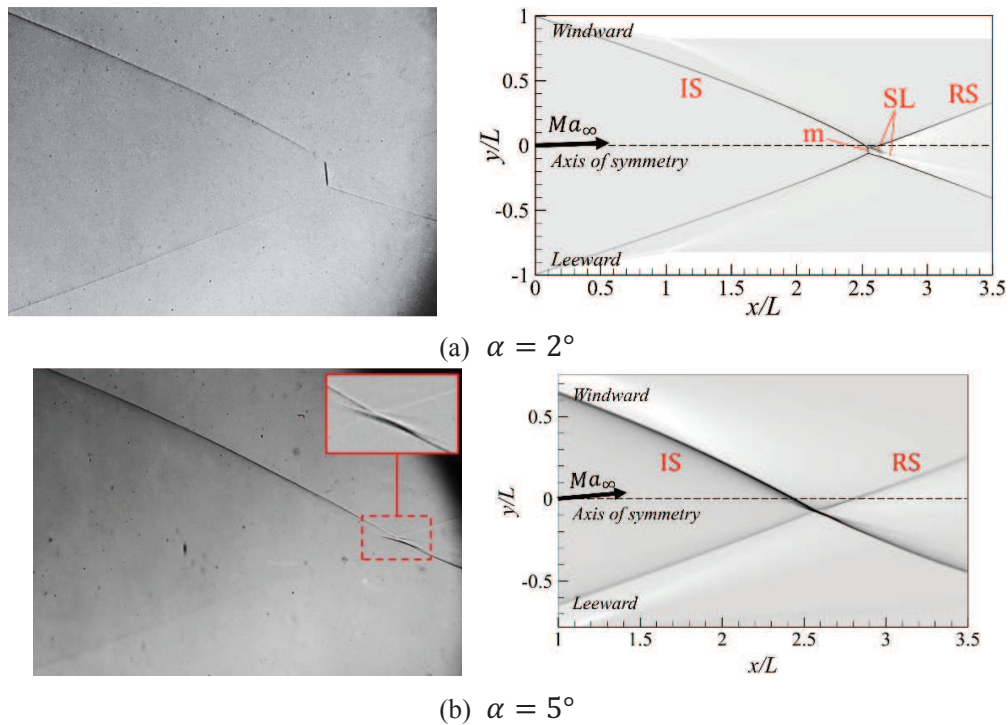


Fig. 11 Experimental (left) and Numerical (right) Schlierens at angles of attack

This part of the works are still at an early stage of the study. Many more cases are needed to be examined in order to obtain extensive characteristics of the non-axisymmetrical effects on a convergent shock wave. In addition, we also realized that the above two simplified models are far from satisfactory for the characterization of the general behaviors of the shock interactions in an inward-turning inlet, and therefore more efforts are planned to be carried out in the future.

5 Concluding remarks

With the help of a couple of simplified models, the complex shock interactions of a hypersonic inward-turning inlet flow are explored and clarified as the interferences dominated by a few key factors, which may provide either understandings of the fundamental mechanisms or some crucial design points for engineering improvement of the performance. Thanks to the advantages of low-cost and high efficiency with simplified models, we expect that more valuable achievements will be obtained as the research steps further.

Acknowledgments The author has to express his deep thanks to Drs. Z. Li, Y. Wu, A. Yu, F. Xiao, D. Wang and Messrs. E. Zhang, Z. Zhang, J. Ji, J. Wang, D. Si for their contributions to the works.

This work was supported by the National Natural Science Foundation of China (Grants Nos. 11872356, 11772325 and 11621202).

References

- [1] A. P. Kothari, C. Tarpley, T. A. McLaughlin, B. S. Babu and J. W. Livingston, *Hypersonic Vehicle Design Using Inward Turning Flow Fields*, 32nd AIAA, ASME, SAE, and ASEE, Joint Propulsion Conference and Exhibit, AIAA, Lake Buena Vista, FL, AIAA-1996-2552
- [2] M. K. Smart, *Design of Three-Dimensional Hypersonic Inlets with Rectangular-to-Elliptical Shape Transition*, Journal of Propulsion and Power, Vol. 15, No. 3, 1999, pp. 408–416
- [3] Y. You, *An Overview of the Advantages and Concerns of Hypersonic Inward Turning Inlets*, 17th AIAA International Space Planes and Hypersonic Systems and Technologies Conference, AIAA, San Francisco, California, AIAA-2011-2269.
- [4] X. Nan and K. Zhang, *Numerical and Experimental Investigation On Hypersonic Inward Turning Inlets with Basic Flowfield Using Arc Tangent Curve Law of Pressure Rise*, 17th AIAA International Space Planes and Hypersonic Systems and Technologies Conference, AIAA, Washington, DC, 2011, AIAA-2011-2270..
- [5] M. K. Smart and C. A. Trexler, *Mach 4 Performance of Hypersonic Inlet with Rectangular-to-Elliptical Shape Transition*, Journal of Propulsion and Power, Vol. 20, No. 2, 2004, pp. 288-293.
- [6] Y. Li, Z. Li, J. Yang et al. *Visualization of Hypersonic Inward-Turning Inlet Flows by Planar Laser Scattering Method*, In: 21st AIAA International Space Planes and Hypersonic Systems and Technologies Conference 2017, Xiamen. AIAA 2017-2358
- [7] K. Mu, D. Zhan, Z. Li, et al. *Surface Tuft Flow Visualization in a Hypersonic Inward Turning Inlet/Isolator Model*, In: 21st AIAA International Space Planes and Hypersonic Systems and Technologies Conference 2017, Xiamen. AIAA2017-2385
- [8] Z. Zhang, Z. Li, R. Huang, and J. Yang, *Experimental investigation of shock oscillations in V-shaped blunt leading edges*. Physics of Fluids, 31(2), 026110 (2019)
- [9] F. Xiao, Z. Li, Z. Zhang, Y. Zhu and J. Yang, *Hypersonic Shock Wave Interactions on a V-Shaped Blunt Leading Edge*, AIAA Journal, Vol. 56, No. 1, 2018, pp. 356-367. doi: 10.2514/1.J055915
- [10] D. Wang, Z. Li, Z. Zhang, N. Liu, J. Yang and X. Lu, *Unsteady shock interactions on V-shaped blunt leading edges*, Physics of Fluids 30(11), 116104 (2018).
- [11] G. Ben-Dor, *Shock reflection phenomenon*, Springer, Berlin, 2007.
- [12] J. Ji, E. Zhang, Z. Li and J. Yang, *Non-axisymmetric effects on a conical converging shock wave with flow inclination*, 32nd International Symposium on Shock Waves (ISSW32), 14-19 July 2019, Singapore.